Computers and Geotechnics 110 (2019) 71–81

Contents lists available at ScienceDirect

Computers and Geotechnics

journal homepage: www.elsevier.com/locate/compgeo

Research Paper

Behaviour of existing tunnel due to new tunnel construction below

Xiang Liu, Qian Fang*, Dingli Zhang, Zhongju Wang

Key Laboratory for Urban Underground Engineering of Ministry of Education, Beijing Jiaotong University, Beijing 100044, China

ARTICLE INFO

Keywords:
New tunnelling below existing tunnel
Winkler model
Superposition method
Tunnel deflection

ABSTRACT

This paper proposed an analytical method to study the mechanical behaviours of the existing tunnel due to new tunnelling below. The coefficient of subgrade reaction of the existing tunnel can be considered as a variation instead of a constant. The resultant deflections of the existing tunnel can be calculated by a superimposed method. The proposed method is verified by the finite element method. The influences of the input parameters on the deflection of the existing tunnel are studied. Based on a below-crossing project in Beijing, the results obtained by our method match well with the monitoring data.

1. Introduction

With the increase of subways constructed in densely built-urban areas, the cases of a new tunnel excavated below the existing tunnel are commonly encountered. The key issues of such adjacent tunnelling project are to guarantee the safety and serviceability of the existing tunnel during new tunnel construction. Due to the inherent complexities of the soil-tunnel interactions, it is a great challenge to study the mechanical behaviours of the existing tunnel. The additional movements of existing tunnel induced by adjacent tunnelling have been reported by some researchers using the field measurements [1–7]. The numerical analyses [8–12] and physical model tests [13–16] are also used as powerful tools to gain insights into the mechanical responses of the existing tunnel.

The analytical method, using the theory of beam on elastic foundation, provides a simple and efficient way to study the interactions between the new and existing tunnels. Some studies [17–20] have been performed to investigate the responses of above-crossing tunnelling on the existing tunnel. It is noted these methods are unavailable for the cases of tunnelling below the existing tunnel. The coefficient of subgrade reaction at and adjacent to the intersection of the existing and new tunnels decrease due to excavation. For a specific case of tunnelling below the existing tunnel without clearance, Liu et al. [21] proposed a superposition method to analyse the mechanical behaviours of the existing tunnel.

To address the general issue of new tunnelling below existing tunnel with clearance, a superposition method based on the theory of beam on elastic foundation are adopted to study the mechanical responses of the existing tunnel. The major contribution of this research is that the coefficient of subgrade reaction along the existing tunnel can be considered as a function instead of a constant. The results obtained by our method are in agreement with those by numerical simulation. Parametric analyses are also performed to study the soil-tunnel interactions on the mechanical behaviours of the existing tunnel. Moreover, the mechanical responses of the existing twin tunnels due to new twin tunnels excavation in Beijing are investigated. The results of the deflections of existing twin tunnels obtained by the proposed method are in accordance with the on-site monitoring data.

2. Analytical solution

2.1. Soil-tunnel interaction model

We aim to study the mechanical responses of the existing tunnel due to new tunnelling below. The calculation model is shown in Fig. 1. The interaction between soil and existing tunnel is modelled by means of a series of closely spaced independent linear springs. The excavation of the new tunnel results in a variation of the stiffness of the springs along the new tunnel. A continuous Euler-Bernoulli beam is used to model the existing tunnel. The unloading pressure $q(x)$ acting on the existing tunnel due to new tunnel construction can be obtained by the unloading load p associated with the new tunnel construction.

2.2. Solution of Winkler foundation model

The governing equation for an infinitely Euler-Bernoulli beam on Winkler foundation is given by:

$$E_bI\frac{d^4W(x)}{dx^4} + KBW(x) = q(x)B \tag{1}$$

* Corresponding author.
E-mail address: qfang@bjtu.edu.cn (Q. Fang).

https://doi.org/10.1016/j.compgeo.2019.02.013
Received 23 August 2018; Received in revised form 3 January 2019; Accepted 12 February 2019

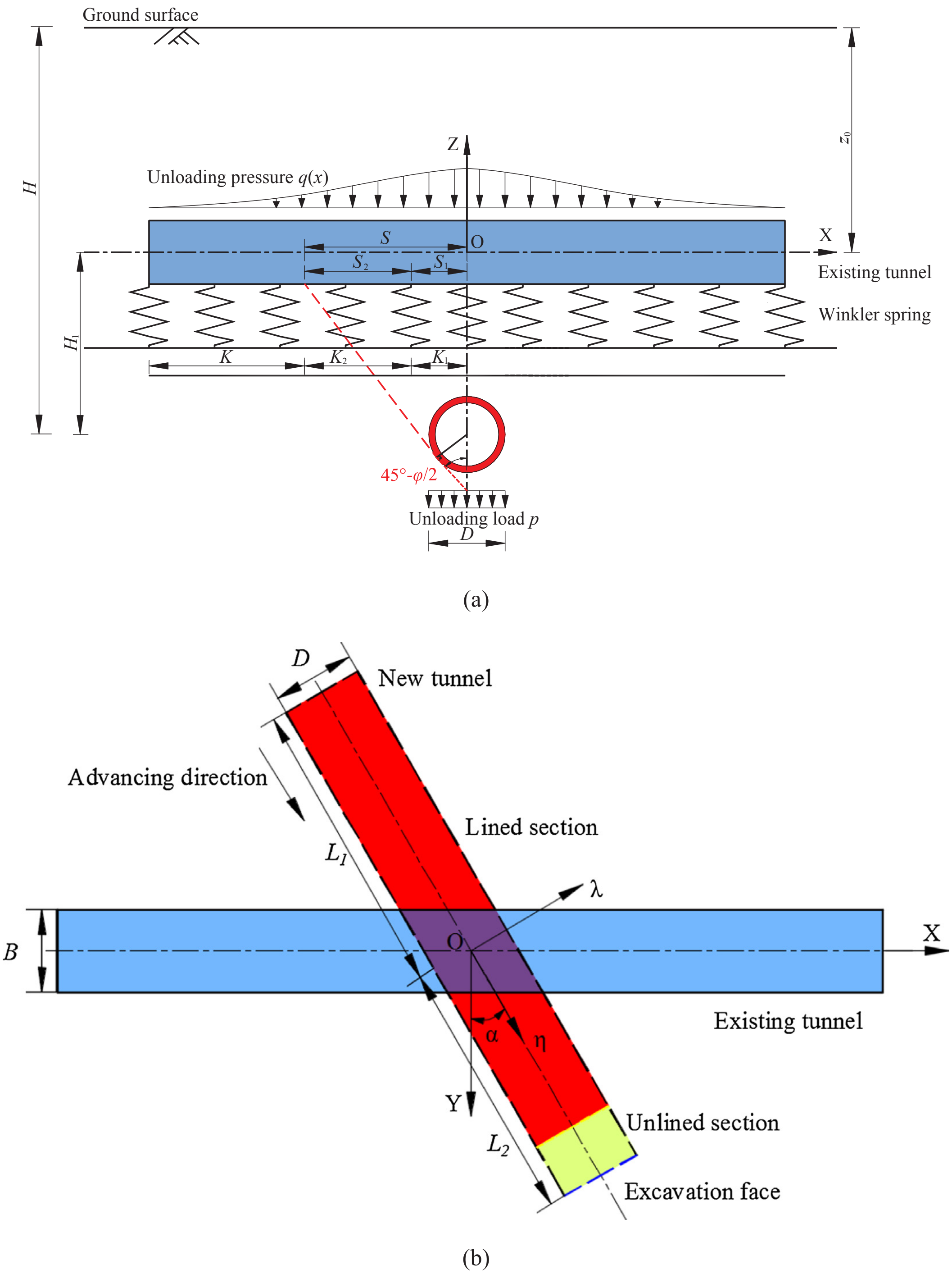

Fig. 1. Model sketch (a) cross section view of new tunnel and (b) plan view.

where E_bI is the equivalent bending stiffness of the beam; $W(x)$ is the deflection of the beam; K is the coefficient of subgrade reaction; B is the cross-sectional width of the beam; and $q(x)$ is the unloading pressure acting on the beam induced by new tunnel construction.

The solution of Eq. (1) can be written as:

$$W(x) = W_0(x) + v(x) \tag{2}$$

where $W_0(x)$ is the general solution of Eq. (1), and $v(x)$ is the particular solution related to the unloading pressure $q(x)$.

The general solution can be written as:

$$W_0(x) = e^{\beta x}(C_1 cos\beta x + C_2 sin\beta x) + e^{-\beta x}(C_3 cos\beta x + C_4 \sin\beta x) \tag{3}$$

where the characteristic of the system $\beta = \sqrt[4]{KB/4E_bI}$. The parameters C_1, C_2, C_3, and C_4 are four integration constants. The constants can be determined by boundary conditions.

Since $e^{\beta x} \to \infty$, $e^{-\beta x} \to 0$ when $x \to \infty$ and $W(x) = 0$ at $x \to \infty$, Eq. (3) can be simplified as:

$$W_0(x) = e^{-\beta x}(C_3 cos\beta x + C_4 \sin\beta x) \tag{4}$$

If a concentrated load P is applied at the origin, the rotation angle $\theta(x)$ is zero and the shear force $Q(x)$ is $-P/2$ at the origin:

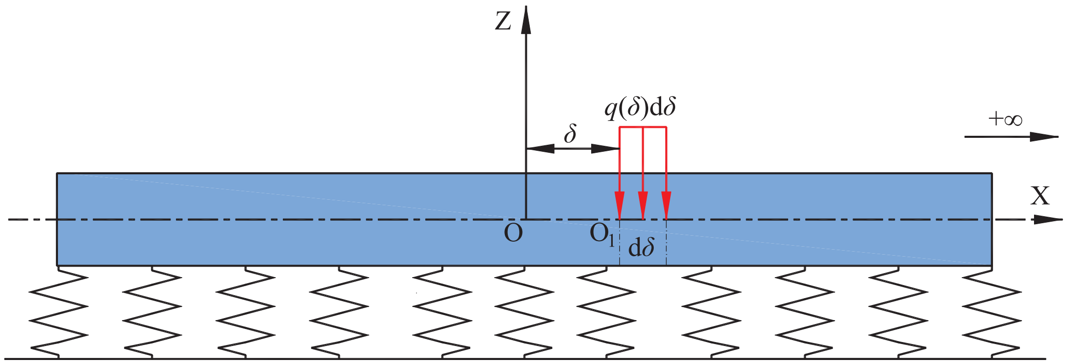

Fig. 2. Winkler foundation model induced by external load $q(\delta)\mathrm{d}\delta$.

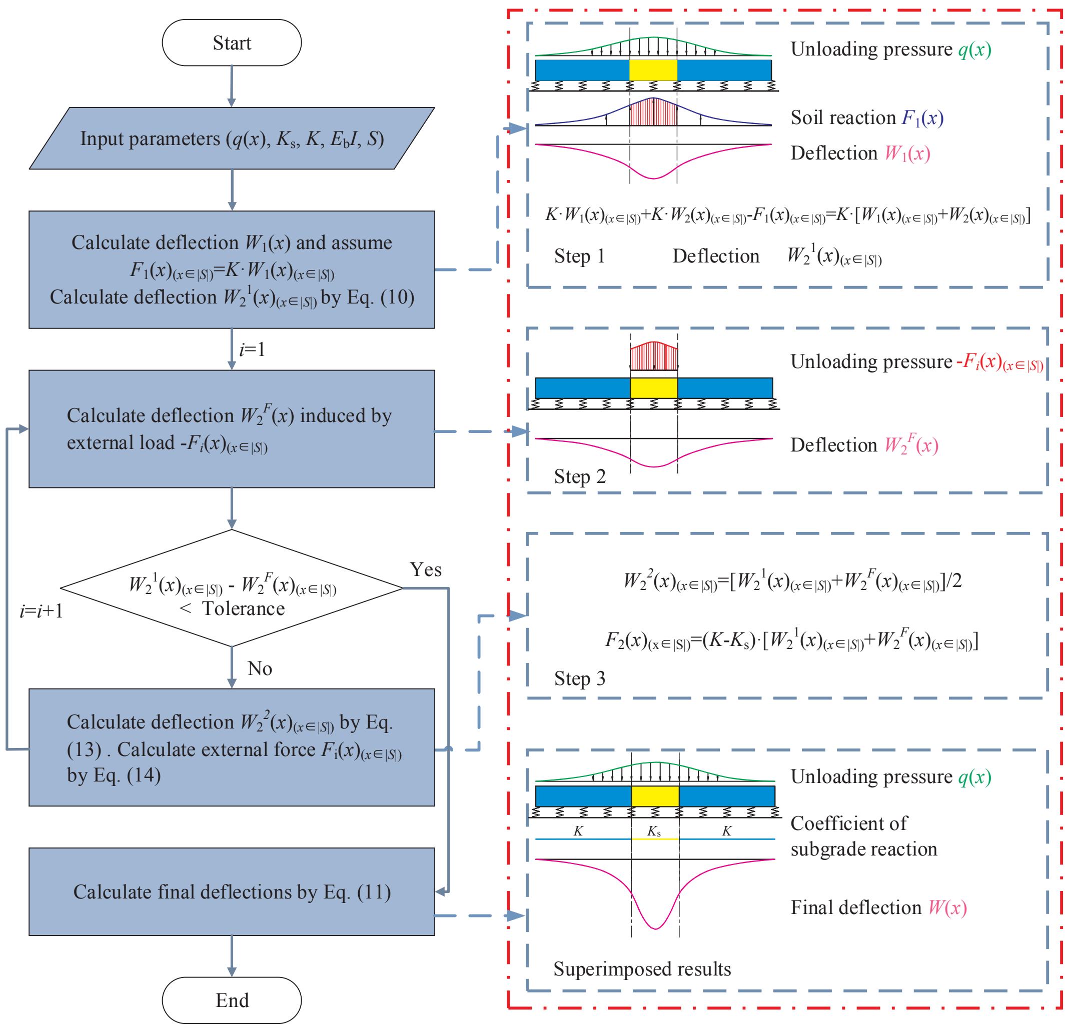

Fig. 3. Superposition method for existing tunnel due to new tunnelling below with clearance.

$$\begin{cases} \theta(x) = \frac{dW_P(x)}{dx}|_{x=0} = 0 \\ Q(x) = -E_bI\frac{d^3W_P(x)}{dx^3}|_{x=0} = -\frac{P}{2} \end{cases} \tag{5}$$

Substituting Eq. (4) into Eq. (5), the constants C_3 and C_4 can be obtained:

$$C_3 = C_4 = \frac{P\beta}{2KB} \tag{6}$$

Consequently, the vertical deflection of the infinite beam induced by a concentrated load P can be expressed as:

$$W_P(x) = \frac{P\beta}{2KB}e^{-\beta x}(cos\beta x + \sin\beta x) \tag{7}$$

When $q(\delta)$ is applied on an infinitesimal element length $d\delta$ at an arbitrary position δ of the infinite beam (Fig. 2), the origin of the infinite beam can be assumed to shift from O to O_1. The resultant deflection $dW(x)$ can be calculated by Eq. (7), in which P is substituted by $q(\delta)Bd\delta$ and x is substituted by $|x-\delta|$, respectively. That is:

$$dW(x) = \frac{q(\delta)d\delta\beta}{2K}e^{-\beta|x-\delta|}(cos\beta\ |x-\delta| + \sin\beta\ |x-\delta|) \tag{8}$$

The general deflection $W(x)$ of the infinite beam caused by

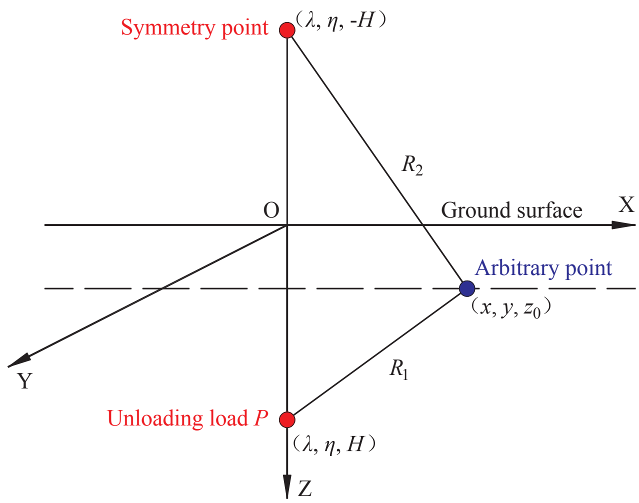

Fig. 4. Unloading pressure caused by unloading load due to excavation.

unloading distributed pressure can be obtained through integrating Eq. (8):

$$W(x) = \int_{-\infty}^{+\infty} \frac{q(\delta)\beta}{2K} e^{-\beta|x-\delta|}(\cos\beta\,|x-\delta| + \sin\beta\,|x-\delta|)d\delta \tag{9}$$

2.3. Calculation process

To consider the variable coefficients of subgrade reaction along the beam of the foundation model, we propose a superposition method to calculate the deflection of the beam. We use the Bisection method to solve the mathematical problem by a series of iterations. The calculation process is shown in Fig. 3.

The sum of the virtue reaction forces ($KW_1(x)_{(x\in|S|)} + KW_2(x)_{(x\in|S|)}$) of each superimposed step subtracting the virtue external load ($F_1(x)_{(x\in|S|)}$) will balance the actual reaction force ($K_s[W_1(x)_{(x\in|S|)} + W_2(x)_{(x\in|S|)}]$) of the beam. The virtue reaction forces are calculated using the classical foundation model considering the coefficient of subgrade reaction along the beam is K. And the actual reaction forces are obtained considering the coefficient of subgrade reaction is K_s from $-S$ to S and the coefficient of subgrade reaction is K at the other sections of the beam. The equilibrium equation can be given by:

$$KW_1(x)_{(x\in|S|)} + KW_2(x)_{(x\in|S|)} - F_1(x)_{(x\in|S|)} = K_s[W_1(x)_{(x\in|S|)} + W_2(x)_{(x\in|S|)}] \tag{10}$$

where $W_1(x)$ is the deflection of the existing tunnel calculated by the unloading pressure $q(x)$; $W_2(x)$ is the deflection of the existing tunnel calculated by the virtual external load $F_1(x)_{(x\in|S|)}$.

The final deflection of the beam from $-S$ to S can be obtained by:

$$W(x)_{(x\in|S|)} = W_1(x)_{(x\in|S|)} + W_2(x)_{(x\in|S|)} \tag{11}$$

In the first step, an initial value of $W_2(x)_{(x\in|S|)}$ can be obtained by substituting $F_1(x)_{(x\in|S|)} = KW_1(x)_{(x\in|S|)}$ into Eq. (10). $W_2^1(x)_{(x\in|S|)}$ can be expressed by:

$$W_2^1(x)_{(x\in|S|)} = \frac{K_s W_1(x)_{(x\in|S|)}}{K - K_s} \tag{12}$$

where the superscript of $W_2(x)_{(x\in|S|)}$ is the order of the iteration in the superimposed process.

Second, $F_1(x)_{(x\in|S|)}$ is applied equally and oppositely as the external load to the beam of the classical elastic foundation model to calculate a new deflection $W_2^F(x)_{(x\in|S|)}$. $W_2^1(x)_{(x\in|S|)}$ can be updated by calculating the mean of the $W_2^1(x)_{(x\in|S|)}$ and $W_2^F(x)_{(x\in|S|)}$. That is:

$$W_2^2(x)_{(x\in|S|)} = \frac{1}{2}[W_2^1(x)_{(x\in|S|)} + W_2^F(x)_{(x\in|S|)}] \tag{13}$$

Third, if the difference between $W_2^1(x)_{(x\in|S|)}$ and $W_2^F(x)_{(x\in|S|)}$ is smaller than a prescribed constant (close to zero), the deflection of the proposed problem $W(x)$ can be obtained by Eq. (11). Or else, $W_2(x)_{(x\in|S|)}$ in Eq. (10) can be replaced by $W_2^2(x)_{(x\in|S|)}$. A new external force $F_2(x)_{(x\in|S|)}$ can be recalculated by substituting $W_2^2(x)_{(x\in|S|)}$ into Eq. (10):

$$F_2(x)_{(x\in|S|)} = (K - K_s)[W_2^2(x)_{(x\in|S|)} + W_1(x)_{(x\in|S|)}] \tag{14}$$

$F_2(x)_{(x\in|S|)}$ is again applied equally and oppositely as the external load to the beam of the classical elastic foundation model to calculate the deflection $W_2^F(x)_{(x\in|S|)}$.

The process is continued until the interval between $W_2(x)_{(x\in|S|)}$ and $W_2^F(x)_{(x\in|S|)}$ is sufficiently small.

Based on the abovementioned calculation process, the coefficient of subgrade reaction can be considered as a function to describe the soil-existing tunnel behaviours due to new tunnel construction below.

For the case of tunnelling below the existing tunnel without clearance, the coefficient of subgrade reaction is zero at and adjacent to the intersection of new and existing tunnels. In such cases, the coefficient of subgrade reaction K_s from -S to S is zero. Substituting $K_s = 0$ into Eqs. (12) and (14), the $W_2^1(x)_{(x\in|S|)}$ and $F_2(x)_{(x\in|S|)}$ can be expressed as:

$$W_2^1(x)_{(x\in|S|)} = 0 \tag{15}$$

Table 1
Input parameters of model.

Parameter	Unit	Value
z_0	m	12.0
H	m	23.6
D	m	6.2
L_1	m	100.0
L_2	m	100.0
S_e	m^2	30.2
S_l	m^2	6.3
γ_s	kN/m^3	16.9
γ_l	kN/m^3	22.5
μ	–	0.3
E_bI	$GPa{\cdot}m^4$	3.8
K	MPa/m	33.4
K_1	MPa/m	23.4 (23.4, 16.7)
K_2	MPa/m	26.7 (26.7, 23.4)
S_1	m	2.0 (3.0, 3.0)
S_2	m	2.0 (3.0, 3.0)

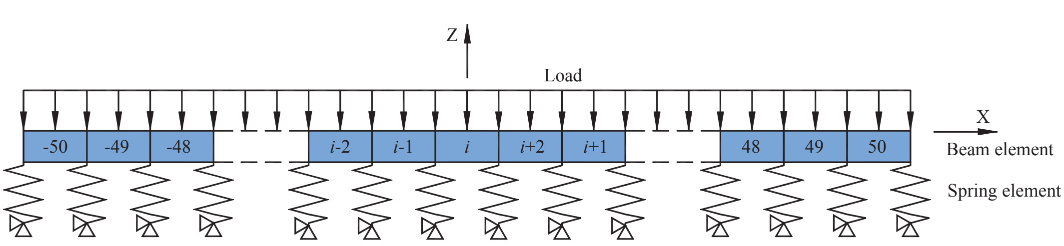

Fig. 5. Numerical model of finite element method.

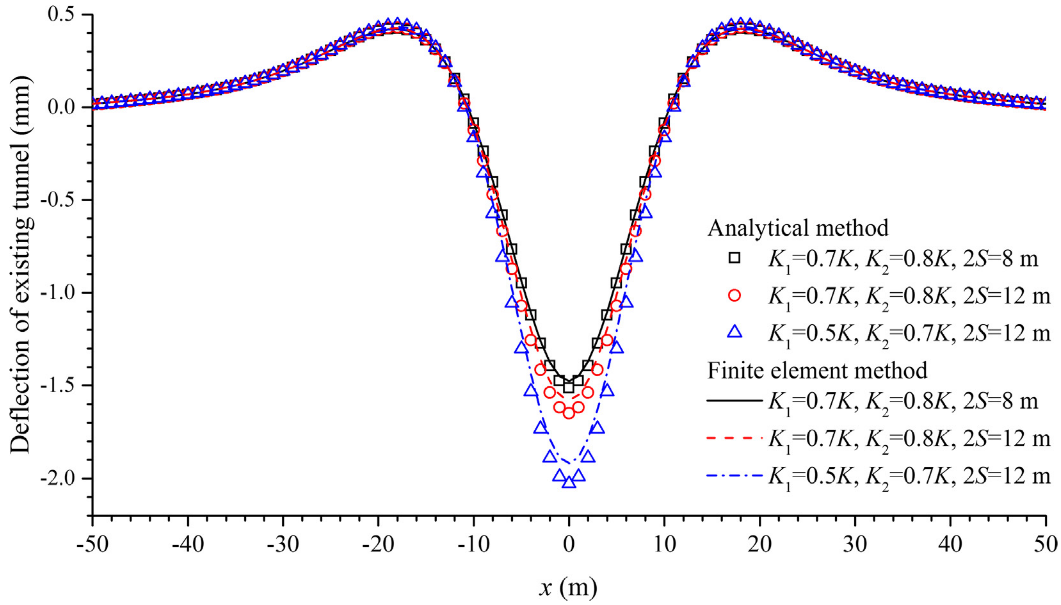

Fig. 6. Deflections calculated by proposed method and finite element method.

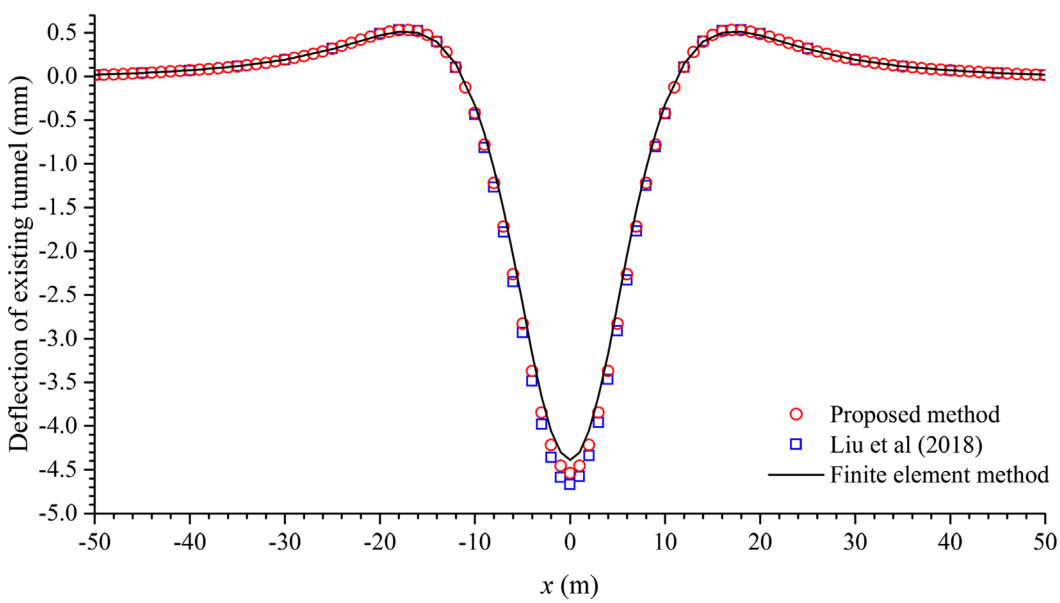

Fig. 7. Comparison of deflections of existing tunnel due to tunnelling below without clearance by different methods.

$$F_2(x)_{(x\in|S|)} = K(W_2^2(x)_{(x\in|S|)} + W_1(x)_{(x\in|S|)}) \tag{16}$$

According to Eq. (11), the deflection of the existing tunnel due to tunnelling below without clearance can be obtained by:

$$W(x)_{K_s=0} = W_1(x) + W_2^F(x)_{K_s=0} \tag{17}$$

2.4. Determination of input parameters

Five input parameters are required to calculate the deflection of the existing tunnel, including the equivalent bending stiffness of the existing tunnel E_bI, the coefficient of subgrade reaction of the undisturbed soil K, the coefficient of subgrade reaction of the disturbed soil K_s, the length of disturbed soil below the existing tunnel $2S$, and the unloading pressure $q(x)$.

2.4.1. Equivalent bending stiffness of existing tunnel

The parameter E_bI is related to the lining type of the existing tunnel. The equivalent bending stiffness of a composite lining can be calculated by the elastic modulus of the lining and the cross-section geometry of the tunnel. The equivalent bending stiffness of a segmental lining is related to the properties of the segments, joints, and bolts. Some theoretical methods have been proposed to study the equivalent bending stiffness of segmental lining tunnel [23–25]. The longitudinal continuous model proposed by Shiba et al. [23] is widely used to calculate the equivalent bending stiffness of the shield tunnel. That is:

$$k_{bo} = E_{bo}A_{bo}/l_{bo} \tag{18}$$

$$\varphi_a + \cot\varphi_a = \pi\left(0.5 + \frac{nk_{bo}l}{E_cA_c}\right) \tag{19}$$

$$E_bI = \frac{\cos^3\varphi_a}{\cos\varphi_a + (\varphi_a + \pi/2)\sin\varphi}E_cI_c \tag{20}$$

where k_b is the elastic stiffness of the longitudinal joint; E_{bo} is the elastic modulus of bolt; A_{bo} is the area of bolt $A_{bo} = \pi r_{bo}^2$; r_{bo} is the radius of

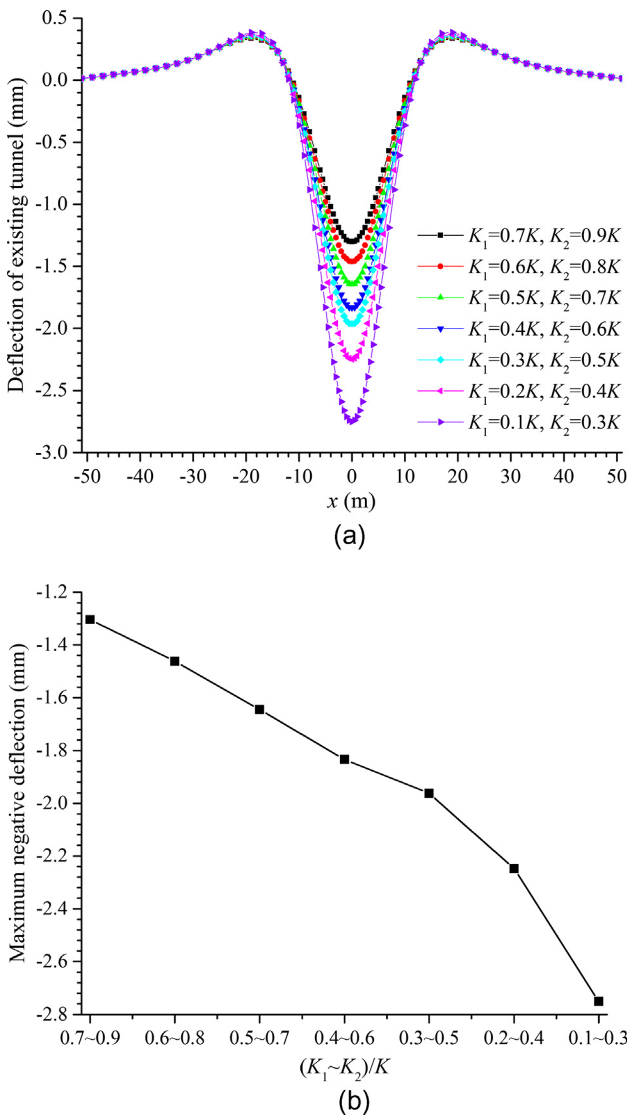

Fig. 8. Deflections of existing tunnel considering different coefficients of subgrade reaction (a) deflections along existing tunnel and (b) maximum negative deflection.

bolt; l_{bo} is the length of bolt; φ_a is the angle of neutral axis; n is the number of longitudinal bolts; l is the width of a tunnel segment; E_c is the elastic modulus of segment; A_c is the sectional area of segments; I_c is the longitudinal inertia moment of the section of a segment.

2.4.2. Coefficient of subgrade reaction

The coefficient of subgrade reaction K, describing the soil-structure interaction, is related to the existing tunnel and the soil underlying and surrounding the existing tunnel. Some empirical and analytical methods have been proposed to estimate the value of K [26–29]. In this research, we use the method proposed by Yu et al. [30] to calculate the coefficient of subgrade reaction, of which the overburden depth of the concerned structure can be considered.

$$K = kB = \frac{3.08}{\eta}\frac{E_s}{1-\mu^2}\sqrt[8]{\frac{E_sB^4}{EI}}$$
$$\eta = \begin{cases} 2.18 & \text{when}\frac{z_0}{B} \leqslant 0.5 \\ 1 + \frac{1}{1.7z_0/B} & \text{when}\frac{z_0}{B} > 0.5 \end{cases} \quad (21)$$

where E_s is the elastic modulus of the soil.

In the cases of tunnelling below the existing tunnel, the coefficient of subgrade reaction of the existing tunnel is not a constant due to the disturbance of the new tunnel excavation. To appropriately consider the mechanical behaviours of the springs at and adjacent to the intersection of the new and existing tunnels, we can use some functions to describe the variation of the coefficient of subgrade reaction along the existing tunnel.

2.4.3. Length of disturbed soil below existing tunnel

The length of disturbed soil below the existing tunnel (2S) can be calculated using the Rankine's earth pressure theory by assuming the angle between the sliding surface and the horizontal plane is 45° + φ/2. The disturbed length of a circular tunnel can be calculated using Eq. (22).

$$2S = 2H_1 - B + D/\sin(45 - \varphi/2) \quad (22)$$

where H_1 is the distance from the axis of the new tunnel to the axis of the existing tunnel; φ is the friction angle of the subsoil of the existing tunnel; D is the diameter of the new tunnel.

2.4.4. Unloading pressure along existing tunnel

The unloading load p (Fig. 1(a)) due to new tunnel excavation can be obtained by the difference between the weight of the excavated soil and the weight of tunnel linings per unit length. That is:

$$p = \begin{cases} \frac{\gamma_s S_e - \gamma_l S_l}{D} \text{ for lined section} \\ \frac{\gamma_s S_e}{D} \text{ for unlined section} \end{cases} \quad (23)$$

where γ_s and γ_l are the unit weights of the soil and the linings per unit length, respectively; and S_e and S_l are the cross-sectional areas of the excavation and the lining, respectively.

Due to the unloading load, the unloading pressure $q(x)$ acting on the existing tunnel can be obtained by the Mindlin's solution [22] shown in Fig. 4. z_0 and H are the distances from the ground surface to the axis of the existing tunnel and to the axis of the new tunnel, respectively; R_1 is the distance from an arbitrary point (x, y, z_0) of the existing tunnel to a point (λ, η, H) of the unloading load p; and R_2 is the distance from the same point (x, y, z_0) to the point (λ, η, $-H$). If there is a skew angle α between the new and the existing tunnels, the coordinate of the arbitrary point (x, y, z_0) can be expressed as ($x$cosα, $x$sinα, z_0) in the λ − η coordinate system. The parameters R_1 and R_2 can be determined by:

$$R_1 = \sqrt{(x\cos\alpha - \lambda)^2 + (x\sin\alpha - \eta)^2 + (z_0 - H)^2} \quad (24)$$

$$R_2 = \sqrt{(x\cos\alpha - \lambda)^2 + (x\sin\alpha - \eta)^2 + (z_0 + H)^2} \quad (25)$$

Consequently, the unloading pressure along the longitudinal direction of the existing tunnel can be given by:

$$q(x) = \int_{-D/2}^{D/2}\int_{L_1}^{L_2}\frac{pd\lambda d\eta}{8\pi(1-\mu)}\left[-\frac{(1-2\mu)(z_0-H)}{R_1^3} + \frac{(1-2\mu)(z_0-H)}{R_2^3} - \frac{3(z_0-H)^3}{R_1^5} - \frac{3(3-4\mu)z_0(z_0+H)^2 - 3H(z_0+H)(5z_0-H)}{R_2^5} - \frac{30Hz_0(z_0+H)^3}{R_2^7}\right] \quad (26)$$

where L_1 and L_2 are the distance from the intersection point O (shown in Fig. 1(b)) to the start of new tunnel and to the face of new tunnel, respectively; μ is the Poisson's ratio of soil.

3. Verification

To verify the proposed model, the analytical results are compared with those obtained from numerical computations. The MATLAB software is used to carry out the computations for the analytical model. The numerical computations are performed by ABAQUS. As shown in Fig. 5, we use 2D beam elements (the beam element length is 1 m) to model the existing tunnel and a series of spring elements to model the elastic foundation. To verify the proposed method, we can change the spring stiffness to simulate various coefficients of subgrade reaction. The length of the numerical beam model is 100 m and the two ends of the

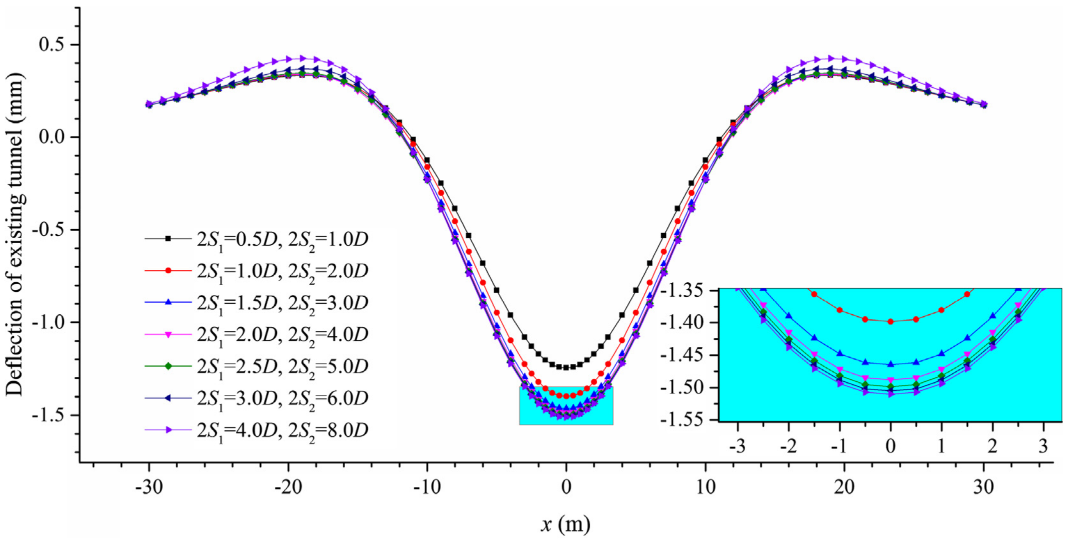

(a)

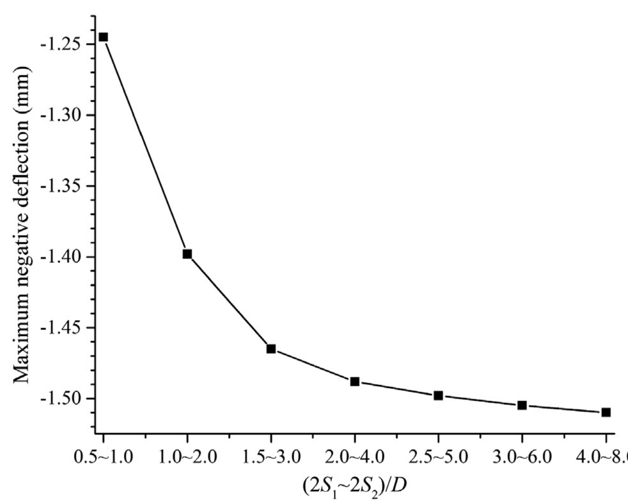

(b)

Fig. 9. Deflections of existing tunnel considering different lengths of disturbed soil (a) deflections along existing tunnel and (b) maximum negative deflection.

model are free. The unloading pressure was calculated by MATLAB and was subsequently applied on the ABAQUS model to solve the problem. The new tunnel is assumed to be excavated perpendicularly below the existing tunnel. The parameters of the three cases used in the verification are shown in Table 1. The resultant deflections of the existing tunnels of the three cases calculated by the proposed method and the finite element method are shown in Fig. 6.

We can see the analytical results agree well with the numerical results. The difference between the analytical result and the numerical result at each point is less than 10%.

For a specific case of new tunnelling below existing tunnel without clearance, the deflections calculated by the proposed method are compared with the deflections obtained by our previous research (Fig. 7) with the same input parameters. The length of disturbed soil $2S$ is 10 m where the spring elements are deleted (the coefficient of subgrade reaction K is zero). The results obtained by different methods are in a good agreement.

4. Parametric analysis

In this section, the main factors influencing the deflection of the existing tunnel, such as the variation coefficient of subgrade reaction, the length of disturbed soil, the horizontal distance between existing and new tunnels, and the vertical clearance between existing and new tunnels, are investigated. The input parameters used in the subsequent analyses are based on the parameters of Case 1 in Section 3.

4.1. Coefficient of subgrade reaction

The deflections of the existing tunnel with different coefficients of subgrade reaction are shown in Fig. 8(a). The coefficient of subgrade reaction K_1 decreases from $0.7\,K$ to $0.1\,K$ and the coefficient of subgrade reaction K_2 decreases from $0.9\,K$ to $0.3\,K$. With the decrease of the coefficient of subgrade reaction, both the maximum positive deflection and the maximum negative deflection of the existing tunnel increase. (Fig. 8(b)).

4.2. Length of disturbed soil

The deflections of the existing tunnel with different lengths of disturbed soil are shown in Fig. 9(a). The curve width increases with the increase of the length of disturbed soil. Meanwhile, the positive deflection of the existing tunnel increases. The maximum negative deflection with different length of disturbed soil is shown in Fig. 9(b). The

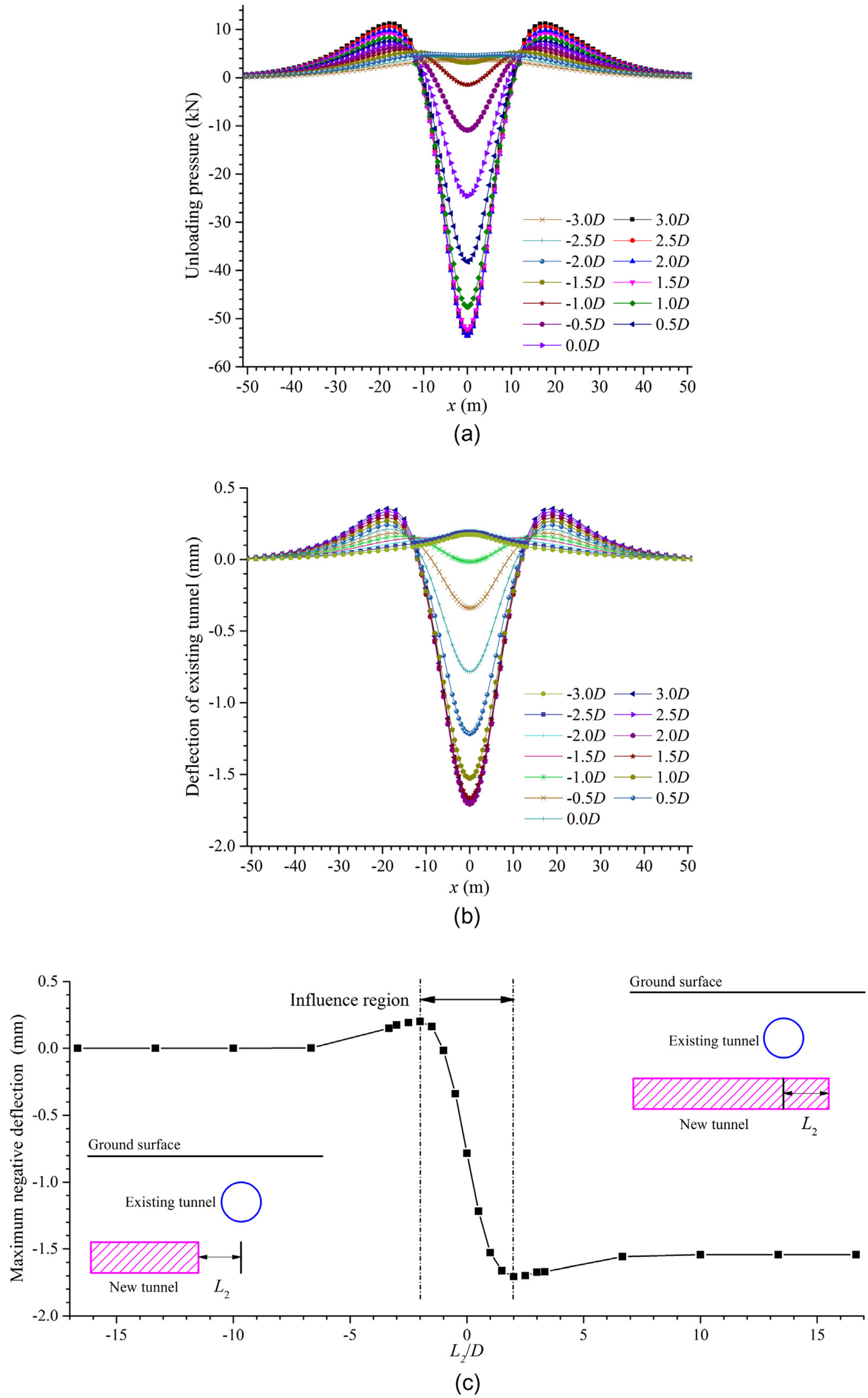

Fig. 10. Unloading pressure and deflections considering different horizontal distances (a) Unloading pressure, (b) Deflections of existing tunnel and (c) Maximum negative deflection of existing tunnel during new tunnel excavation.

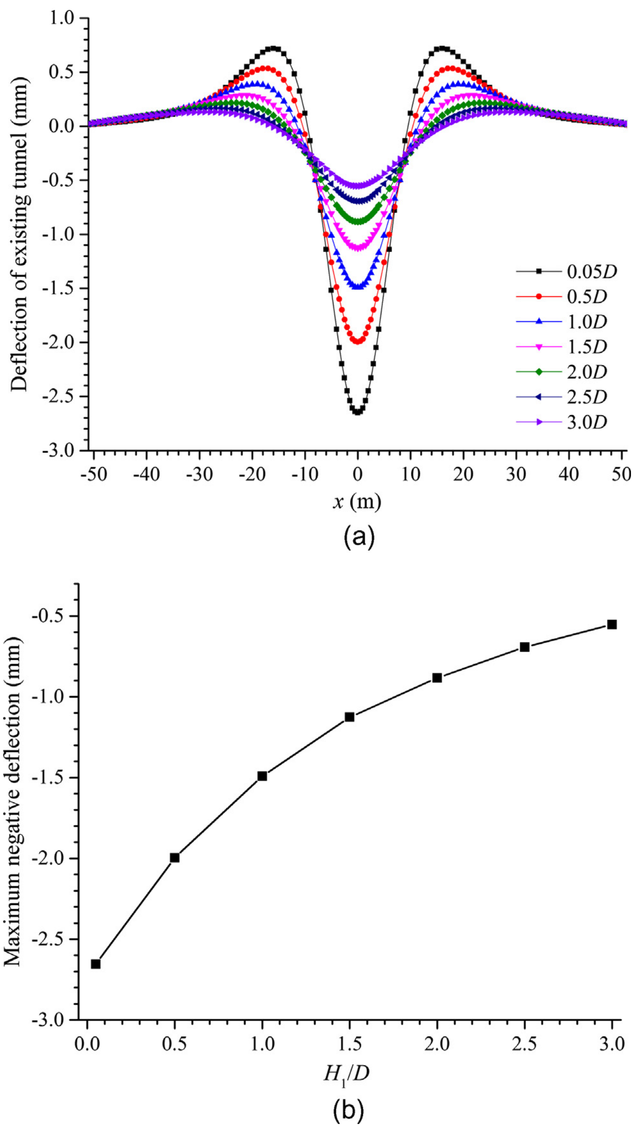

Fig. 11. Deflections of existing tunnel considering different vertical clearances (a) deflections of existing tunnel and (b) maximum negative deflection.

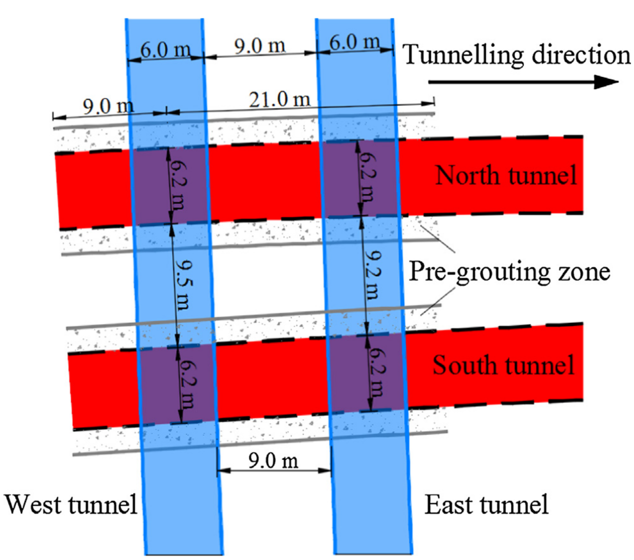

Fig. 12. Plan view.

magnitude of the maximum negative deflection increases with the increase of the length of disturbed soil.

4.3. Horizontal distance between existing and new tunnels

The horizontal distance of the new tunnel face to the axis of the existing tunnel L_2 ranges from -18 m to $+18$ m. The minus sign of L_2 denotes the excavation face is behind the existing tunnel and the plus sign means the excavation face is beyond the existing tunnel.

The unloading pressures during new tunnel excavation with different horizontal distances between the new and existing tunnels are shown in Fig. 10(a). The unloading pressure at the origin is positive and increases slightly from $L_2 = -3D$ to $L_2 = -2D$. Then, the unloading pressure at the origin turns to negative and the magnitude of the maximum negative pressure increases rapidly from $L_2 = -2D$ to $L_2 = +2D$. When L_2 is from $+2D$ to $+3D$, the magnitude of negative unloading pressure decreases.

The deflections of the existing tunnel during the new tunnel excavation are shown in Fig. 10(b). The characteristics of the deflection curves are similar to those of the unloading pressure curves. The maximum negative deflection of the existing tunnel with different horizontal distances between the new and existing tunnels is shown in Fig. 10(c). The maximum negative deflection of the existing tunnel from $L_2 = -2D$ to $L_2 = +2D$ is considerably sensitive to the horizontal distance between the new and existing tunnel. The deflection of existing tunnel changes slightly when the new excavation face is 2D behind or beyond the centreline of the existing tunnel. The curve levels off when the distance L_2 is more than a certain value.

4.4. Vertical clearance between new and existing tunnels

The deflections of the existing tunnel with different vertical clearances are shown in Fig. 11(a). The magnitudes of both the negative deflection and the positive deflection increase with the decrease of the vertical clearance. The maximum negative deflection with different vertical clearances is shown in Fig. 11(b). The magnitude of the maximum negative deflection decreases with the increase of the vertical clearance.

5. Case study

The proposed method can analyse not only the cases of one tunnel crossing below the other, but also the cases of multiple tunnels crossing below multiple tunnels. In this section, the proposed method is used to calculate the mechanical responses of the existing twin tunnels due to new twin tunnels construction in Beijing. The calculation results are compared with the field monitoring data.

5.1. Project overview and calculation parameters

Fang et al. [6] presented a case of closely spaced twin tunnels excavated below the other closely spaced existing twin tunnels of Beijing subway. The plan view of the project and the cross-sectional view of the new twin tunnels are shown in Figs. 12 and 13, respectively. The existing circular shaped twin tunnels are parts of the Beijing subway Line 4. They were excavated by the earth pressure balance shield and they are horizontally parallel. The parameters of the segmental lining are shown in Table 2. The new horseshoe shaped twin tunnels are parts of the Beijing subway Line 6. They were excavated by the shallow tunnelling method. The layout of the monitoring points along the existing twin tunnels is shown in Fig. 13. A hydrostatic level system was adopted to monitor the settlements of the monitoring points set up along the invert of each tunnel. A Hydrostatic level cell was installed at each monitoring point. We used the central monitoring system to record the signals at 30-min intervals. Details can be found in our previous research [6].

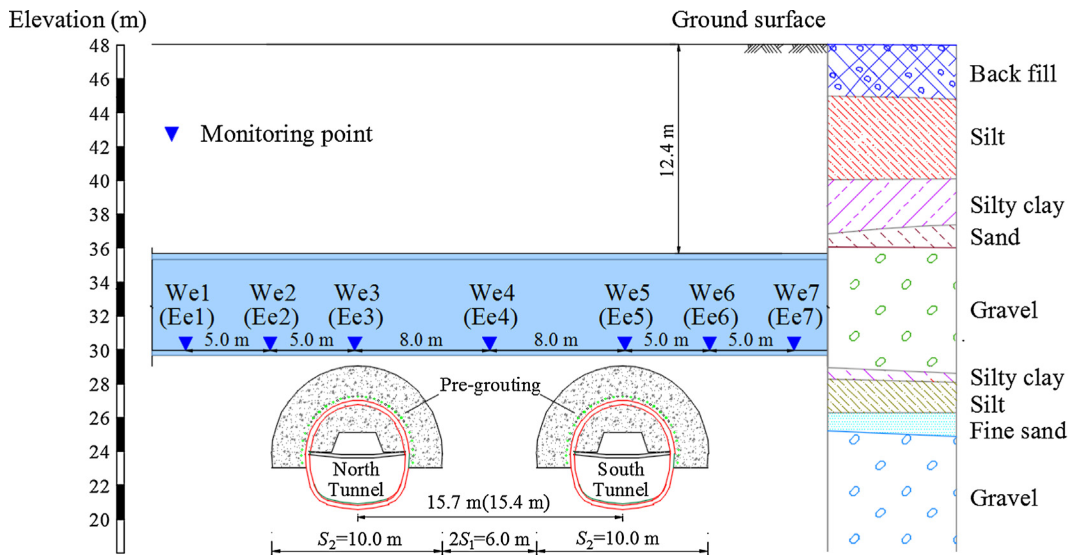

Fig. 13. Cross-section view of new twin tunnels and layout of monitoring points.

Table 2
Tunnel structure parameters.

Parameter	Unit	Value
External diameter B	m	6.0
Segment Width l	m	1.2
Elastic modulus of segment E_c	MPa	3.45×10^4
Number of bolts n	–	17
Bolt diameter r_{bo}	mm	30
Bolt Length l_{bo}	mm	400
Elastic modulus of bolt E_{bo}	MPa	2.06×10^5

Table 3
Calculation parameters.

Parameter	Unit	Value
z_0	m	15.4
H_1	m	2.6
S_1	m	3.0
S_2	m	10.0
K	MPa/m	33.4
K_1	MPa/m	40.1
K_2	MPa/m	13.4
L_1	m	9.0 (24.0)
L_2	m	21.0 (6.0)

The new and existing twin tunnels are mainly located in gravel. The soils between the new and existing tunnels are silty clay, silt, and fine sand. The soils surrounding and inside the top headings of the new twin tunnels are reinforced before the new tunnel excavation, which in turn increase the coefficient of subgrade reaction of the pillar between the twin tunnels. Due to new tunnel excavation, the soils above the excavation are disturbed. The coefficient of subgrade reaction of the soil above the new tunnel decreases. Our paper aims to predict the deformation of existing tunnel at stable stage neglecting the influence of excavation process. In the application, we assume the new twin tunnels are excavated simultaneously to simplify the problem without considering the influences on parameters' identification of each other due to construction. The calculation parameters are shown in Table 3.

5.2. Comparison between monitoring data and analytical results

We use the data of the finial stage (stable stage) to validate our proposed method. The field monitoring data of the final settlement of the existing twin tunnels and the analytical results obtained by our method are shown in Fig. 14. Three different combinations of the coefficient of subgrade reaction along the existing tunnel are considered.

The settlement profiles of the existing twin tunnels, calculated by our method considering the variation of the coefficient of subgrade reaction ($K_2(x)$ and $K_3(x)$), display a double-trough "W" shape, which matches well with the field monitoring results. It is noted that in the analytical study, the new twin tunnels are excavated simultaneously. Therefore, the settlement profile obtained by the analytical study is symmetrical with respect to the centreline of the twin tunnels. But in the real project, due to the complicated interactions of the new twin tunnelling, a larger settlement was reported above the north tunnel, which was first excavated.

To appropriately investigate the mechanical behaviours of the existing tunnel due to new tunnel construction, further studies should be carried out to determine the magnitude and distribution of the coefficient of subgrade reaction, especially the effects of excavation process on the coefficient of subgrade reaction.

6. Conclusions

This paper presents an analytical method to evaluate the mechanical behaviours of the existing tunnel due to new tunnelling below. The existing tunnel is considered as a continuous Euler-Bernoulli beam resting on the Winkler foundation model. The unloading pressure acting on the existing tunnel is calculated by the Mindlin's solution. The coefficient of subgrade reaction of the existing tunnel can be considered as a function instead of a constant. A superimposed method is proposed to calculate the mechanical behaviours of the existing tunnel due to new tunnelling below. The proposed method is successfully verified by numerical analysis.

Parameter analyses using the proposed method are carried out to study the mechanical behaviours of the existing tunnel due to new tunnelling below. With the decrease of the coefficient of subgrade reaction and the vertical clearance between new and existing tunnels, and with the increase of the length of disturbed soil, the magnitude of maximum negative deflection of the existing tunnel increases. The maximum deflection of the existing tunnel is sensitive to the horizontal distance between new and existing tunnel when the new tunnel face is adjacent to the intersection of new and existing tunnels.

Compared with the results calculated by the classical method, the deflections of the existing tunnel calculated by the proposed method

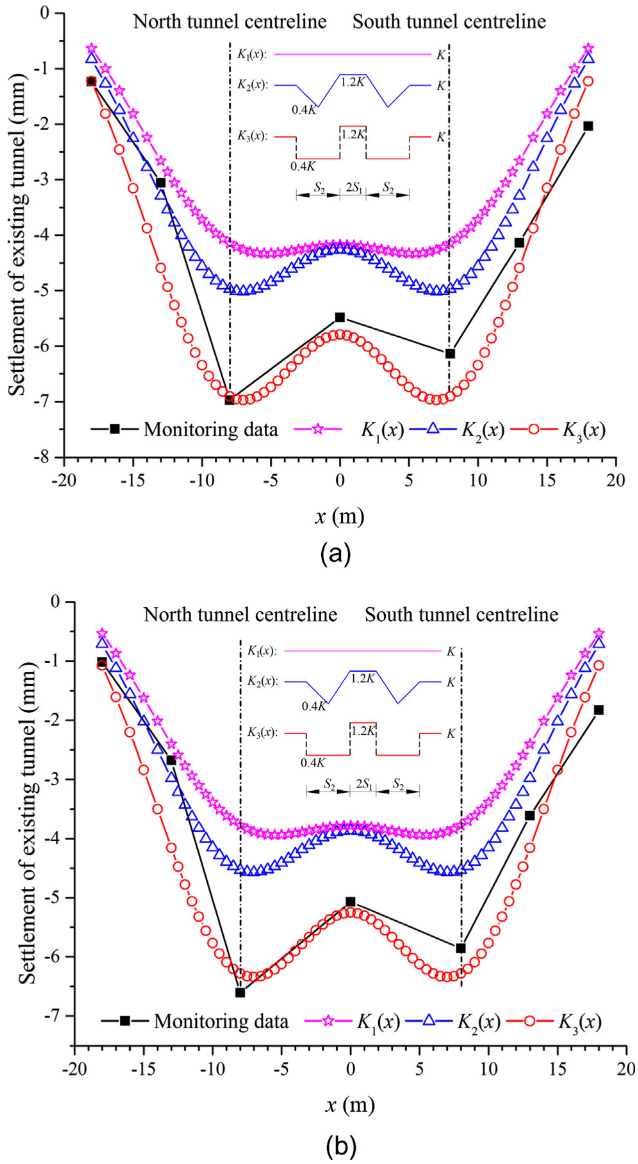

Fig. 14. Measured and calculated settlements with different combinations of coefficients of subgrade reaction (a) west tunnel and (b) east tunnel.

considering the variation of the coefficients of subgrade reaction are in accordance with the monitoring data at stable stage.

Acknowledgements

The authors gratefully acknowledge the financial support by the Fundamental Research Funds for the Central Universities under Grant 2016JBZ009 and Chinese National Natural Science Foundation under Grant 51678035.

References

[1] Kimmance JP, Lawrence S, Hassan O, Purchase NJ, Tollinger G. Observations of deformations created in existing tunnels by adjacent and cross cutting excavations. Proc Geotech Asp Undergr Constr Soft Ground 1996:707–12.
[2] Standing JR, Selman R. The response to tunnelling of existing tunnels at Waterloo and Westminster. Building response to tunnelling: case studies from construction of the Jubilee Line Extension. London: Thomas Telford Publishing; 2001. p. 509–46. 29.
[3] Cooper ML, Chapman DN, Rogers CDF, Chan AHC. Movements in the Piccadilly Line tunnels due to the Heathrow Express construction. Géotechnique 2002;52(4):243–57. https://doi.org/10.1680/geot.52.4.243.41019.
[4] Mohamad H, Bennett PJ, Soga K, Mair RJ, Bowers K. Behaviour of an old masonry tunnel due to tunnelling-induced ground settlement. Géotechnique 2010;60(12):927–38. https://doi.org/10.1680/geot.8.p.074.
[5] Li XG, Yuan DJ. Response of a double-decked metro tunnel to shield driving of twin closely under-crossing tunnels. Tunn Undergr Sp Tech 2012;28:18–30. https://doi.org/10.1016/j.tust.2011.08.005.
[6] Fang Q, Zhang DL, Li QQ, Wong LNY. Effects of twin tunnels construction beneath existing shield-driven twin tunnels. Tunn Undergr Sp Tech 2015;45:128–37. https://doi.org/10.1016/j.tust.2014.10.001.
[7] Gue CY, Wilcock MJ, Alhaddad MM. Monitoring the behaviour of an existing royal mail tunnel: London underground bond street station upgrade works. Geotech Front 2017:525–35. https://doi.org/10.1061/9780784480441.055.
[8] Addenbrooke TI, Potts DM. Twin tunnel interaction: surface and subsurface effects. Int J Geomech 2001;1(2):249–71. https://doi.org/10.1061/(asce)1532-3641(2001)1:2(249).
[9] Chehade FH, Shahrour I. Numerical analysis of the interaction between twin-tunnels: influence of the relative position and construction procedure. Tunn Undergr Sp Tech 2008;23(2):210–4. https://doi.org/10.1016/j.tust.2007.03.004.
[10] Chakeri H, Hasanpour R, Hindistan MA, Unver B. Analysis of interaction between tunnels in soft ground by 3D numerical modeling. Bull Eng Geol Environ 2011;70(3):439–48. https://doi.org/10.1007/s10064-010-0333-8.
[11] Do NA, Dias D, Oreste P, Djeran-Maigre I. Three-dimensional numerical simulation of a mechanized twin tunnels in soft ground. Tunn Undergr Sp Tech 2014;42:40–51. https://doi.org/10.1016/j.tust.2014.02.001.
[12] Avgerinos V, Potts DM, Standing JR. Numerical investigation of the effects of tunnelling on existing tunnels. Géotechnique 2017;67(9):808–22. https://doi.org/10.1680/jgeot.sip17.p.103.
[13] Kim SH, Burd HJ, Milligan GWE. Model testing of closely spaced tunnels in clay. Géotechnique 1998;48(3):375–88. https://doi.org/10.1680/geot.1998.48.3.375.
[14] Ng CWW, Boonyarak T, Masin D. Three-dimensional centrifuge and numerical modeling of the interaction between perpendicularly crossing tunnels. Can Geotech J 2013;50(9):935–46. https://doi.org/10.1139/cgj-2012-0445.
[15] Ng CWW, Wang R, Boonyarak T. A comparative study of the different responses of circular and horseshoe-shaped tunnels to an advancing tunnel underneath. Geotech Lett 2016;6(2):168–75. https://doi.org/10.1680/jgele.16.00001.
[16] Boonyarak T, Ng CWW. Three-dimensional influence zone of new tunnel excavation crossing underneath existing tunnel. Japanese Geotech Soc Special Public 2016;2(42):1512–8. https://doi.org/10.3208/jgssp.hkg-09.
[17] Zhang JF, Chen JJ, Wang JH, Zhu YF. Prediction of tunnel displacement induced by adjacent excavation in soft soil. Tunn Undergr Sp Tech 2013;36:24–33. https://doi.org/10.1016/j.tust.2013.01.011.
[18] Zhang ZG, Huang MS, Wang WD. Evaluation of deformation response for adjacent tunnels due to soil unloading in excavation engineering. Tunn Undergr Sp Tech 2013;38:244–53. https://doi.org/10.1016/j.tust.2013.07.002.
[19] Liang RZ, Xia TD, Hong Y, Yu F. Effects of above-crossing tunnelling on the existing shield tunnels. Tunn Undergr Sp Tech 2016;58:159–76. https://doi.org/10.1016/j.tust.2016.05.002.
[20] Liang RZ, Xia TD, Huang MS, Lin C. Simplified analytical method for evaluating the effects of adjacent excavation on shield tunnel considering the shearing effect. Comput Geotech 2017;81:167–87. https://doi.org/10.1016/j.compgeo.2016.08.017.
[21] Liu X, Fang Q, Zhang DL. Mechanical responses of existing tunnel due to new tunnelling below without clearance. Tunn Undergr Sp Tech 2018;80:44–52. https://doi.org/10.1016/j.tust.2018.06.001.
[22] Mindlin RD. Force at a point in the interior of a semi-infinite solid. Physics 1936;5(7):195–202. https://doi.org/10.1063/1.1745385.
[23] Shiba Y, Kawashima K, Obinata N, et al. Evaluation method of longitudinal stiffness of shield tunnel linings for application to seismic response analysis. Proc Jpn Soc Civil Eng. 1988;398:319–27. https://doi.org/10.2208/jscej.1988.398_319. (in Japanese).
[24] Shiba Y, Kawashima K. Evaluation procedure for seismic stress developed in shield tunnels based on seismic deformation method. Proceedings of the Japan Society of Civil Engineering 1989. p. 385–94. https://doi.org/10.2208/jscej.1989.404_385. (in Japanese).
[25] He C. A study on the seismic behavior in the longitudinal direction of shield tunnels. The Dissertation for the degree of Ph.D. Tokyo: Waseda University; 1999. (in Japanese).
[26] Biot MA. Bending of an infinite beam on an elastic foundation. Zeitschrift fiir Angewandte Maihematik und Mechanik 1922;2(3):165–84.
[27] Vesic AS. Bending of beams resting on isotropic elastic solid. J. Soil Mech. Found. Eng., ASCE. 1961;87(2):35–53.
[28] Attewell PB, Yeates J, Selby AR. Soil Movement induced by tunnelling and their effects on pipelines and structures. London: Blackie and Son Ltd.; 1986.
[29] Klar A, Vorster TEB, Soga K, Mair RJ. Soil-pipe interaction due to tunnelling: comparison between Winkler and elastic continuum solutions. Géotechnique 2005;55(6):461–6. https://doi.org/10.1680/geot.2005.55.6.461.
[30] Yu J, Zhang CR, Huang MS. Soil–pipe interaction due to tunnelling: assessment of Winkler modulus for underground pipelines. Comput Geotech 2013;50:17–28. https://doi.org/10.1016/j.compgeo.2012.12.005.